TENSILE PROPERTIES OF AEROGEL-BASED CARBON NANOTUBE/ POLY (VINYL ALCOHOL) COMPOSITE FIBERS

Jialin Liu[1], Cuixia Zhang[1], Shuxuan Qu[1], Qingwen Li[1] and Weibang Lu[1]*

[1] Division of Advanced Nanomaterials, Suzhou Institute of Nano-Tech and Nano-Bionics, CAS
No. 398 Ruoshui Road, Suzhou 215123, China
Email: wblv2013@sinano.ac.cn, web page: http://www.sinano.cas.cn/

Keywords: Carbon nanotube fiber, Polymer infiltration, Interface, Mechanical property

ABSTRACT

High-performance fiber development is a persistent key theme in the field of composite materials. The one-dimensional assemblies of individual carbon nanotubes (CNTs), which are known as CNT fibers, have unprecedented properties and are expected to be revolutionary fiber materials. These CNT fibers can be fabricated using a one-step floating catalyst chemical vapor deposition method, which can be ready scaled up for industrial fabrication. This method yields aerogel-based CNT fibers in which the CNTs have diameters of several nanometers and lengths of several hundred micrometers to 1 millimeter. These high aspect ratios result in a large amount of CNT interweaving and cause high porosity and inefficient intertube-load transfer within the fiber. Accordingly, the tensile mechanical properties of the current CNT fibers remain inferior to these of advanced carbon fibers and individual CNTs. In this study, we aimed to strengthen CNT fibers by enhancing the inter-tube load transfer efficiency via infiltration with polyvinyl alcohol and by improving the packing density and alignment of both CNTs and polymer chains using densification and hot-stretching treatments. The tensile strengths of the fibers increased from 470.2 MPa to 1.2 GPa, and the tensile modulus increased from 14.9 GPa to 36.7 GPa, suggesting the promise of these materials for the construction of high-performance structural composites.

1 INTRODUCTION

Carbon nanotubes (CNTs) possess superb mechanical, electrical, and thermal properties. For example, the tensile moduli and strengths of individual CNTs are approximately 1 TPa and 50 to 100 GPa, respectively [1, 2], and these materials have electrical and thermal conductivities that are comparable to or even better than those of metal materials. Accordingly, CNTs have been recognized as promising reinforcements for high-performance and multifunctional composite materials. Because the mechanical properties of fiber-reinforced composites depend greatly on both the content and alignment of fillers and their interactions with matrix materials, the past two decades have seen great efforts to introduce CNTs evenly throughout composites and align them in the desired directions. To date, the best solution involves the assembly of aligned CNTs into fibers, followed by the use of these fibers as reinforcements in the composites. Currently, CNT fibers can be spun from a CNT solution [3], a CNT film drawn from a pre-grown vertically aligned CNT array [4], or a CNT aerogel synthesized in a high-temperature furnace [5].

Although few studies have shown that the tensile strength of CNT fibers can be over 8 GPa when testing very short or ultrathin samples [6, 7], the reported tensile mechanical properties of these fibers remain far inferior to those of high-performance carbon fibers [8]. This is primarily attributed to the high aspect ratios of CNTs, which cause waving and interweaving and result in high porosities and inefficient intertube load transfers within fibers [9]. Several densification methods, such as liquid densification, fiber twisting, die draw-through, and mechanical compression [10-14], have been adopted to overcome these challenges. Although the porosities of CNT fibers were somewhat reduced, the load transfers between CNTs were still mediated via weak van der Waals interactions. Accordingly, some researchers have aimed to establish stronger covalent bonding between CNTs using tube e-beam or ion beam irradiation or surface functionization [15]. Unfortunately, these approaches destroyed the structures of CNTs and thus degraded their mechanical and electrical properties [16, 17].

Alternatively, polymer infiltration offers a simple and effective method for reinforcing CNT fibers without destroying the CNT structures. Polymer networks within a fiber not only enhance the load transfer between neighboring CNTs, but also establish new connections between distant CNTs [18]. To date, several types of polymers, such as polyvinyl alcohol (PVA), polyimide, and epoxy, have been adopted to reinforce array-spun CNT fibers [19-21]. For example, aerogel-spun CNT fibers have drawn recent and increasing attention because of their readiness for industry fabrication [8]. Few preliminary studies have attempted to reinforce aerogel-spun CNT yarns through polymer infiltration. For example, Jung et al. [22] reported that the tensile strengths and moduli of aerogel-based CNT yarns could be effectively enhanced by infiltrating three kinds of polymers: polystyrene, polyacrylonitrile, and PVA. The infiltration of PVA—the polymer with the poorest affinity toward CNTs—yielded the greatest improvements in the mechanical and electrical properties of CNT fibers.

In this work, we developed a new method of strengthening aerogel-based CNT fibers using PVA infiltration accompanied by post-densification and hot-stretching treatment. We selected PVA because it is a thermoplastic resin with a high level of toughness and a large number of hydrogen bonds [23] and is very effective for reinforcing CNT fibers [18, 22]. Die draw-through and hot-stretching were subsequently implemented to enhance the packing density and alignment of both the PVA chains and CNTs in the fiber. We also performed a preliminary study of the structure–tensile property relationship.

2 MATERIALS AND METHODS

2.1 Fabrication of the aerogel-based CNT ribbon

A CNT aerogel was synthesized using the floating catalyst chemical vapor deposition (FCCVD) method and supplied by Suzhou Creative Nano Carbon Co., Ltd. The details of this process can be found in Ref [24]. Briefly, the feeding stock, a mixture of ethanol (carbon source), ferrocene (catalyst precursor), and thiophene (promoter), was injected into a high-temperature tube furnace, using a mixture of hydrogen and argon gases as the carrier. CNTs were synthesized within the furnace and entangled with each other to form a sock-like CNT aerogel. This aerogel was continuously blown out from the furnace and shrunk into a ribbon after passing through a water bath. This ribbon was continuously extruded and wound onto a rotating roller. The winding process stretched the aerogel and roughly aligned the CNTs in the drawing direction. In this study, the thickness and width of the CNT ribbon were approximately 21 μm and 1.5 to 1.7 mm, respectively.

2.2 PVA infiltration into the CNT ribbon

PVA (molecular weight 205000 $g \cdot mol^{-1}$, Mowiol 224) was supplied by Shanghai Aladdin Bio-Chem Technology Co., Ltd and dissolved in deionized water at room temperature while stirring. The CNT/PVA composites were fabricated by placing CNT ribbons into a PVA solution and allowing them to soak sufficiently at 85 ℃ for 3 h. To explore the influence of the PVA content on the tensile properties of fibers, solutions with various PVA concentrations (0.125, 0.25, 0.5, and 1 wt%) were prepared. Notably, the original CNT ribbon was too weak to be drawn out from a solution with a higher PVA concentration.

2.3 Densification and stretching of the CNT/PVA composite fiber

To enhance the packing densities and alignments of PVA chains and CNTs, composite ribbons were drawn through a series of dies with successively decreasing hole diameters (300, 200, 180, 150, 130, 120, and 100 μm) to yield fibers with circular cross-sections. Next, the fibers were hot-stretched using a universal testing machine (E44.104, MTS) equipped with a heating chamber (GDX200). Specifically, a 10-cm-long fiber sample was clamped in the heating chamber at temperatures ranging from 100 ℃ to 160 ℃ and was stretched at a rate of 0.01 mm/s. The stretching process was suspended when the fiber elongation reached 1.0 mm and repeated once the tensile force was saturated until the fiber failed. The failed fibers were then characterized to evaluate the effect of hot-stretching.

2.3 Characterization

The mechanical properties of fibers were tested on a mechanical testing machine (Instron 3365). The tensile testing rate was 1 mm/min, and the gauge length was 10 mm. Thermogravimetric (TG) analyses were performed using a TG analyzer (TG 209 F1 Libra, NETZSCH) at a heating rate of 10 K/min. Dynamic mechanical analysis (DMA) was performed using a DMA 242 E Artemis (Netzsch). The tests were conducted at room temperature, an operating frequency of 1 Hz, a force amplitude of 0.2 N, and a displacement amplitude of 80 μm. The surface morphology was observed using a scanning electron microscope (SEM, Hitachi S4800).

3 RESULTS AND DISCUSSION

3.1 Structure and tensile performance of a pure CNT fiber

The sock-like CNT aerogel synthesized using the FCCVD method shrunk into a ribbon-like filament upon entering the water. TG tests were performed in both air and nitrogen atmospheres to quantitatively evaluate the content of impurities in the dried CNT ribbons. As shown in Fig. 1A, the ribbon was calculated to contain 5.5% amorphous carbon and 8.6% Fe. The surface morphology of the CNT ribbon is shown in Fig. 1B and demonstrates the formation of small, curly bundles that entangle with each other. The interspaces between CNTs or CNT bundles ranged from several nanometers to several hundred nanometers, far beyond the van der Waals interaction distances, thus limiting the load transfer between neighboring CNTs. Next, ribbons were drawn through dies with decreasing hole diameters to densify the network. As shown in Fig. 1C, most CNTs aligned along the drawing direction, although a few voids remained among the CNT bundles. It should be noted that although the diameter of the last die is 80 μm, the diameter of the obtained CNT fiber was 95 to 100 μm. This may be attributable to the radial elastic recovery of the CNT fiber after passing through the die [12].

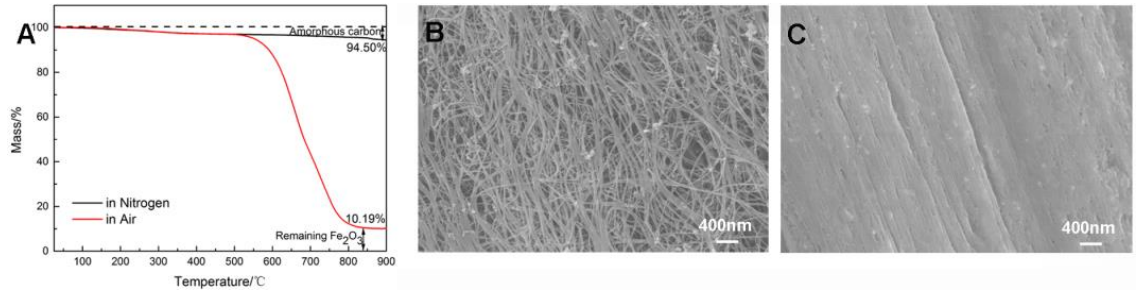

Figure 1: (A) Impurity content of CNT ribbon. Morphologies of CNT ribbons before (B) and after (C) being drawn through dies observed by SEM.

The tensile mechanical properties of CNT fibers were evaluated using a single-fiber tensile test. The tensile strength and modulus of the densified CNT fiber were approximately 470.2 ± 48.3 MPa and 14.9 ± 1.9 GPa, respectively, and the fail strain is approximately 21.3 ± 2.5%. A representative stress–strain curve can be found in Fig. 2A.

3.2 Effect of the PVA composition

To further enhance the intertube load transfer in the fiber, the CNT ribbon was first immersed in a PVA solution, and the resulting composite ribbons were drawn through several dies with decreasing diameters. To reveal the effect of the PVA content on the mechanical properties of composite fibers, a series of fibers were made by varying the PVA content in the solution—0.125, 0.25, 0.5, and 1.0 wt%. The PVA contents of the final composite fibers were evaluated through TG analyses (Fig. 2B), which yielded values of 17.4 wt%, 19.1 wt%, 22.3 wt%, and 30.7 wt% respectively. Single-fiber tensile testing was also performed to study the tensile mechanical properties of the CNT/PVA composite fibers. Table 1 summarized the tensile strengths, moduli, and failure strains of fibers with varying PVA concentrations. The representative stress–strain curves of all fibers are also shown in Fig. 2A.We observed that the tensile strengths and moduli of the fibers increased with increasing PVA concentration. This was not surprising, because the increased PVA could fill more of the intertube

spaces in the fiber. Fig. 2C and 2D depict the surface morphologies of composite fibers that contain 0.5 wt% and 1 wt% PVA, respectively. As shown clearly, the former fiber still contains some free voids, whereas most of these were filled with PVA in the latter fiber. Greater amounts of PVAs in the interspaces of CNTs can effectively enhance the load transfer efficiency between neighboring CNTs. Notably, the shear between the die hole and fiber forced a better alignment of CNTs on the fiber surface in the axial direction, as shown in Figs. 2C and 2D. The tensile strength and modulus of a fiber containing 30.7 wt% PVA were approximately 749.2 ± 46.7 MPa and 16.5 ± 0.6 GPa, respectively, which was 59.3% and 14.9% higher than that of a pure CNT fiber, respectively.

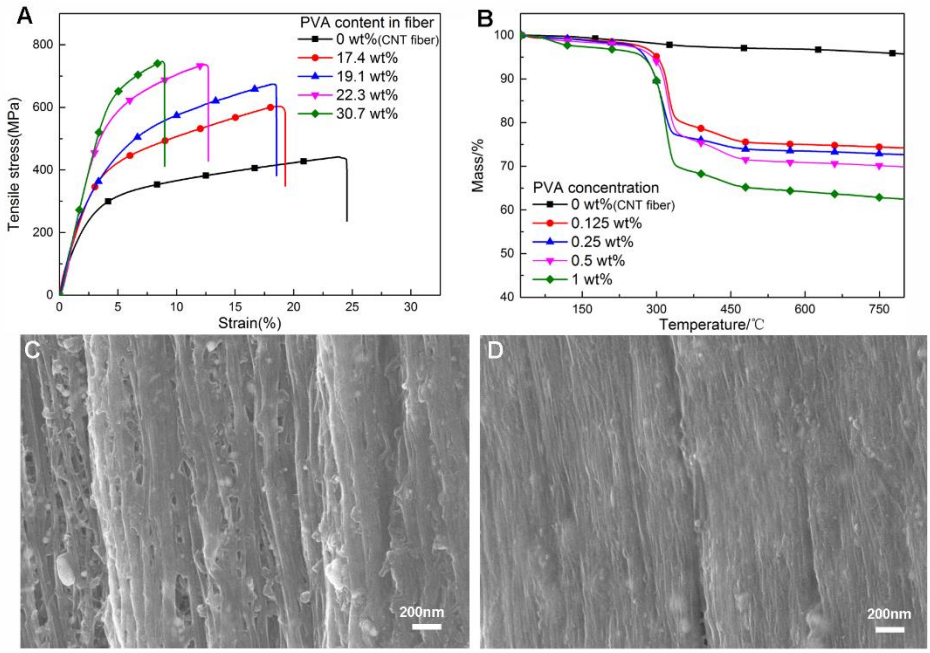

Figure 2: (A) TG and (B) stress-strain curves of CNT fibers and CNT/PVA composite fibers with different PVA contents. Morphologies of CNT/PVA composite fibers containing 22.3 wt% (C) and 30.7 wt% (D) PVA.

PVA concentration in solution [wt%]		0	0.125	0.25	0.5	1
PVA content in fiber [wt%]		0	17.4	19.1	22.3	30.7
d [μm]	BHS	95.0 ±4.5	86.8 ±5.1	90.0 ±4.4	89.2 ±8.8	85.5 ±5.3
	AHS	110.0 ±1.0	91.8 ±6.5	95.5 ±1.0	89.5 ±5.1	80.4 ±4.8
σ [MPa]	BHS	470.2 ±48.3	619.2 ±29.6	695.2 ±21.0	741.0 ±67.3	749.2 ±46.7
	AHS	221.9 ±28.3	984.8 ±46.0	934.4 ±57.0	962.3 ±75.4	1182.8 ±83.3
E [GPa]	BHS	14.9 ±1.9	17.0 ±1.5	17.5 ±0.6	17.2 ±1.4	16.5 ±0.6
	AHS	7.7 ±0.6	28.4 ±3.7	26.5 ±1.7	29.4 ±2.8	36.7 ±2.5
ε [%]	BHS	21.3 ±2.5	12.2 ±5.8	21.5 ±4.9	15.2 ±3.4	11.3 ±4.4
	AHS	7.1 ±1.1	5.1 ±0.8	5.3 ±0.5	6.3 ±0.2	4.9 ±0.5

Table 1. Masses of PVA and mechanical properties of PVA/CNT composite fibers before hot-stretching (BHS) and after hot-stretching (AHS). *d*, *σ*, *E*, and *ε* represent the fiber diameter, tensile stress, tensile modulus, and tensile strain, respectively.

3.3 Effect of stretching

Post-stretching is widely used in the traditional fiber industry. This process can greatly increase the alignment of polymer chains in the fiber direction and thus enhance the mechanical performance of fibers. In this context, the obtained CNT/PVA composite fibers were stretched in a hot furnace to further increase the alignment and densification of CNTs within the fibers.

Fig. 3 depicts the internal structure evolution of the composite fiber. In the first step, polymer infiltration, PVA was either absorbed on the surfaces of CNTs or into the free interspaces between CNTs comprising the ribbon. Both CNTs and PVA chains were curly and entangled with each other to yield a loosely packed composite ribbon. After passing through a series of dies, the ribbon was transformed into a fiber with enhanced packing density. The diameter of the CNT/PVA fibers was less than that of the final die, in contrast to the pure CNT fibers as discussed earlier. PVA chains in the composite fiber restrict the elastic recovery of a CNT network passed through the dies, and the evaporation of intermolecular water during the drying process led to a decrease in fiber diameter. During hot-stretching, the temperature was set above the T_g but lower the T_m of PVA to facilitate PVA chain mobility. Upon stretching, both the CNTs and PVA chains were forced to align along the direction of tension. Given the viscoelasticity of PVA, stretching was suspended for periods of time to allow the fiber to equilibrate and deform evenly. In this study, the fibers were stretched by 12% to 20%.

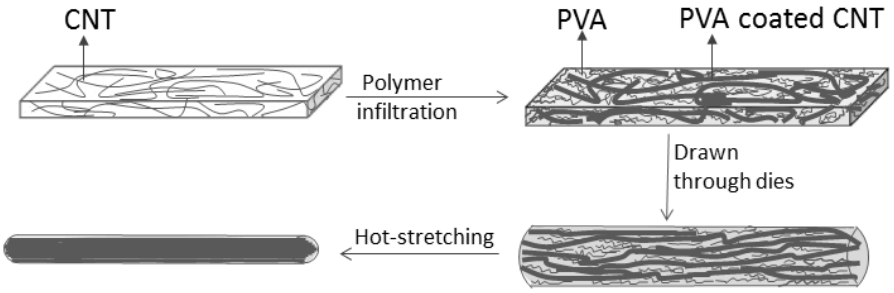

Figure 3: Schematics of the internal structure evolution during the fabricating CNT/PVA composite fiber fabrication.

The tensile properties of pure CNT fibers and composite fibers after hot-stretching are compared in Fig. 4A and Table 1. The tensile strength of the CNT fibers decreased from 470.2 ± 48.3 MPa to 221.9 ± 28.3 MPa, and the modulus decreased from 14.9 ± 1.9 GPa to 7.7 ± 0.6 GPa. This reduction may be attributable to the radial thermal expansion of CNT fibers in the hot environment, as indicated by the increase in diameter (Fig. 4B). Radial looseness within the CNT fiber degrades the intertube load transfer efficiency and reduces the tensile strength and modulus. However, hot-stretching effectively enhanced both the tensile strengths and moduli of all CNT/PVA composite fibers. For example, the tensile strength and modulus of composite fibers containing 30.7 wt% PVA increased to 1.2 ± 0.1 GPa and 36.7 ± 2.5 GPa, respectively, which was 57.9% and 122.0% higher than those of the unstretched counterparts, and 151.6% and 146.3% higher than those of pure CNT fibers, respectively.

Interestingly, the diameters of pure CNTs fibers and composite fibers containing 17.4 wt%, 19.1 wt%, and 22.3 wt% PVA increased after hot-stretching whereas the diameter of composite fibers containing 30.7 wt% PVA decreased, indicating the dichotomous effect of hot-stretching. On one hand, the fiber expands upon heating, which increases the diameter. On the other hand, stretching tends to induce radial shrinkage due to the Poisson effect. The diameter of a hot-stretched fiber depends on the balance of these two phenomena. For composite fibers with 30.7 wt% PVA, the latter effect overwhelms the former, whereas the former effect is dominant for the other fibers.

Fig. 4C compares the loss factor and the ratio of loss modulus to storage modulus of the pure CNT fibers, CNT/PVA composite fibers, and hot-stretched CNT/PVA composite fibers. Here, the loss factor of the pure CNT fiber was much higher than those of the composite fibers and hot-stretched composite fibers. In the pure fibers, the CNTs entangled with each other. Upon loading, the entangled

CNTs unwound and energy dissipated as a result of unrecoverable intertube sliding. In the CNT/PVA composite fibers, the PVA network in the fiber restricted sliding between CNTs and most of the energy was stored by the elastic deformation of PVA, thus reducing the loss factor. Here, energy dissipated mainly through PVA chain sliding and CNT/PVA interface debonding. Hot-stretching enhanced the alignment of both CNTs and PVA chains in the fiber direction and rendered the fibers stronger and stiffer. Therefore, upon loading and unloading, the fiber experienced a majorly elastic deformation of PVA and CNTs, which further reduced the loss factor. Meanwhile, the loss factors of all fibers decreased over time, suggesting that cyclic loading/unloading would enhance the recoverability of these fibers.

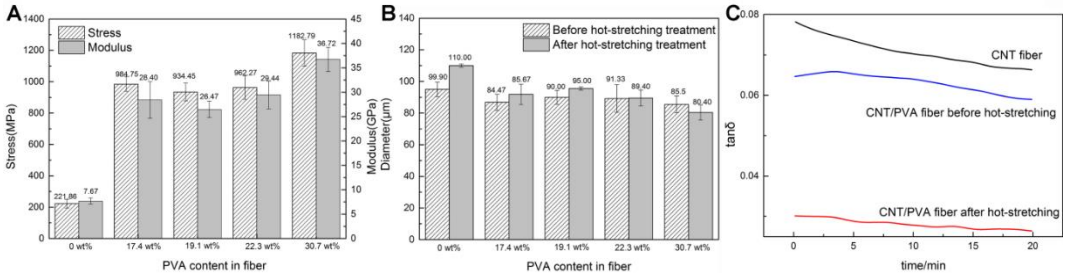

Figure 4: The tensile properties (A) and diameters (B) of CNT fiber and CNT/PVA composite fibers. (C) Variations in fiber loss factors with testing time.

4 CONCLUSIONS

In summary, we developed an efficient method to reinforce aerogel-based CNT fibers via PVA infiltration, followed by densification and hot-stretching. PVA filled the free spaces in CNT fibers and enhanced the load transfer between neighboring CNTs, thus increasing the tensile properties of fibers at the macro-scale. Subsequent passage through a series of dies with decreasing diameters increased the density of the fibers and enhanced the load transfer between CNTs and PVA. We also found that the fiber strength increased with the PVA content for composite fibers containing 0 to 30.7 wt% PVA. Lastly, hot-stretching of the composite fibers increased the alignment of both CNTs and PVA chains along the fiber direction, which further strengthened the composite fibers. Fibers with 30.7 wt% PVA had tensile strengths and moduli as high as 1.2 ± 0.1 GPa and 36.7 ± 2.5 GPa, respectively, or approximately 151.6% and 146.3% higher, respectively, than those of pure CNT fibers.

We note that although the CNT fibers were greatly strengthened by the processes developed in this study, the fiber strength remains far inferior to those of currently used high-performance fibers. To further increase the fiber strength and fully transfer the superb properties of individual CNTs to microscale fibers, further research efforts are needed, possibly including optimization of the interface between CNTs and PVA and efforts to increase the mechanical performance of PVA itself through crystallization. These studies are undergoing and will be reported in the future.

ACKNOWLEDGEMENT

WBL acknowledges the support received from the National Natural Science Foundation of China (Grant No.11472291) and the Natural Science Foundation of Jiangsu Province (Grant No. SBK2014020568).

REFERENCES

[1] M.-F. Yu, B. S. Files, S. Arepalli and R. S. Ruoff, Tensile Loading of Ropes of Single Wall Carbon Nanotubes and their Mechanical Properties, *Physical Review Letters,* 84, 2000, 5552-5.

[2] M.-F. Yu, O. Lourie, M. J. Dyer, K. Moloni, T. F. Kelly and R. S. Ruoff, Strength and Breaking Mechanism of Multiwalled Carbon Nanotubes Under Tensile Load, *Science,* 287, 2000, 637.

[3] B. Vigolo, A. Pénicaud, C. Coulon, C. Sauder, R. Pailler, C. Journet, P. Bernier and P. Poulin, Macroscopic Fibers and Ribbons of Oriented Carbon Nanotubes, *Science,* 290, 2000, 1331.
[4] M. Zhang, K. R. Atkinson and R. H. Baughman, Multifunctional Carbon Nanotube Yarns by Downsizing an Ancient Technology, *Science,* 306, 2004, 1358.
[5] H. W. Zhu, C. L. Xu, D. H. Wu, B. Q. Wei, R. Vajtai and P. M. Ajayan, Direct Synthesis of Long Single-Walled Carbon Nanotube Strands, *Science,* 296, 2002, 884.
[6] K. Koziol, J. Vilatela, A. Moisala, M. Motta, P. Cunniff, M. Sennett and A. Windle, High-Performance Carbon Nanotube Fiber, *Science,* 318, 2007, 1892-5.
[7] W. Xu, Y. Chen, H. Zhan and J. N. Wang, High-Strength Carbon Nanotube Film from Improving Alignment and Densification, *Nano Lett,* 16, 2016, 946-52.
[8] W. Lu, M. Zu, J. H. Byun, B. S. Kim and T. W. Chou, State of the Art of Carbon Nanotube Fibers: Opportunities and Challenges, *Adv Mater,* 24, 2012, 1805-33.
[9] M. Naraghi, T. Filleter, A. Moravsky, M. Locascio, R. O. Loutfy and H. D. Espinosa, A Multiscale Study of High Performance Double-Walled Nanotube−Polymer Fibers, *ACS Nano,* 4, 2010, 6463-76.
[10] L. Kai, S. Yinghui, Z. Ruifeng, Z. Hanyu, W. Jiaping, L. Liang, F. Shoushan and J. Kaili, Carbon Nanotube Yarns with High Tensile Strength Made by a Twisting and Shrinking Method, *Nanotechnology,* 21, 2010, 045708.
[11] X. Zhang, Q. Li, Y. Tu, Y. Li, J. Y. Coulter, L. Zheng, Y. Zhao, Q. Jia, D. E. Peterson and Y. Zhu, Strong Carbon-Nanotube Fibers Spun from Long Carbon-Nanotube Arrays, *Small,* 3, 2007, 244-8.
[12] K. Sugano, M. Kurata and H. Kawada, Evaluation of Mechanical Properties of Untwisted Carbon Nanotube Yarn for Application to Composite Materials, *Carbon,* 78, 2014, 356-365.
[13] J. N. Wang, X. G. Luo, T. Wu and Y. Chen, High-Strength Carbon Nanotube Fibre-Like Ribbon with High Ductility and High Electrical Conductivity, *Nature Communications,* 5, 2014, 3848.
[14] G. Liu, Y. Zhao, K. Deng, Z. Liu, W. Chu, J. Chen, Y. Yang, K. Zheng, H. Huang, W. Ma, L. Song, H. Yang, C. Gu, G. Rao, C. Wang, S. Xie and L. Sun, Highly Dense and Perfectly Aligned Single-Walled Carbon Nanotubes Fabricated by Diamond Wire Drawing Dies, *Nano Letters,* 8, 2008, 1071-5.
[15] S. W. Kim, T. Kim, Y. S. Kim, H. S. Choi, H. J. Lim, S. J. Yang and C. R. Park, Surface Modifications for the Effective Dispersion of Carbon Nanotubes in Solvents and Polymers, *Carbon,* 50, 2012, 3-33.
[16] H. Dai, E. W. Wong and C. M. Lieber, Probing Electrical Transport in Nanomaterials: Conductivity of Individual Carbon Nanotubes, *Science,* 272, 1996, 523.
[17] L. Valentini, S. B. Bon and J. M. Kenny, Anisotropic Electrical Transport Properties of Aligned Carbon Nanotube/PMMA Films Obtained by Electric-Field-Assisted Thermal Annealing, *Macromolecular Materials and Engineering,* 293, 2008, 867-71.
[18] K. Liu, Y. Sun, X. Lin, R. Zhou, J. Wang, S. Fan and K. Jiang, Scratch-Resistant, Highly Conductive, and High-Strength Carbon Nanotube-Based Composite Yarns, *ACS Nano,* 4, 2010, 5827-34.
[19] J. Sandler, M. S. P. Shaffer, T. Prasse, W. Bauhofer, K. Schulte and A. H. Windle, Development of a Dispersion Process for Carbon Nanotubes in an Epoxy Matrix and the Resulting Electrical Properties, *Polymer,* 40, 1999, 5967-71.
[20] A. Allaoui, S. Bai, H. M. Cheng and J. B. Bai, Mechanical and Electrical Properties of a MWNT/Epoxy Composite, *Composites Science and Technology,* 62, 2002, 1993-8.

[21] P. Liu, T. Q. Tran, Z. Fan and H. M. Duong, Formation Mechanisms and Morphological Effects on Multi-Properties of Carbon Nanotube Fibers and their Polyimide Aerogel-Coated Composites, *Composites Science and Technology,* 117, 2015, 114-20.
[22] Y. Jung, T. Kim and C. R. Park, Effect of Polymer Infiltration on Structure and Properties of Carbon Nanotube Yarns, *Carbon,* 88, 2015, 60-9.
[23] J. Meng, Y. Zhang, K. Song and M. L. Minus, Forming Crystalline Polymer-Nano Interphase Structures for High-Modulus and High-Tensile/Strength Composite Fibers, *Macromolecular Materials and Engineering,* 299, 2014, 144-53.
[24] Y. L. Li, I. A. Kinloch and A. H. Windle, Direct Spinning of Carbon Nanotube Fibers from Chemical Vapor Deposition Synthesis, *Science,* 304, 2004, 276-8.